applied sciences

MDPI

Article

Mechanical Behavior of a Mine Tailing Stabilized with a Sustainable Binder

Hamid Reza Manaviparast [1], João Pinheiro [1], Elmira Khaksar Najafi [2], Cláudia Abreu [1], Nuno Araújo [1], Nuno Cristelo [3] and Tiago Miranda [4,*]

[1] Department of Civil Engineering, University of Minho, 4800-058 Guimarães, Portugal
[2] Department of Engineering, University of Trás-os-Montes e Alto Douro, 5000-801 Vila Real, Portugal
[3] School of Science and Technology, University of Trás-os-Montes e Alto Douro, 5000-801 Vila Real, Portugal
[4] ISISE, ARISE, Department of Civil Engineering, University of Minho, 4800-058 Guimarães, Portugal
* Correspondence: tmiranda@civil.uminho.pt

Abstract: Mining is a primary sector for the national economy of many countries, but exploiting these natural resources causes negative impacts on the environment. Tailings produced during mining, called mine tailings, have to be disposed of, and for that purpose, they are often mixed with Portland cement to control environmental toxicity and improve their mechanical properties. However, the high environmental impacts of producing Portland cement are well known. In this sense, sustainable binders based on the alkaline activation of industrial wastes have been studied as an alternative to using Portland cement. This study focused on applying a sustainable binder based on the alkaline activation of fly ash to improve the mechanical performance of a mine tailing from a mine located in Portugal. Geotechnical tests and chemical analysis were conducted to characterize the mine tailing and fly ash used in the alkaline activation process. In addition, triaxial tests were performed to evaluate the mechanical performance of the specimens, with both natural and stabilized tailings. The developed study proved that stabilized tailing with activated fly ash shows promising mechanical performance showing that this approach can be an excellent alternative to using Portland cement.

Keywords: mine tailing; alkaline activation; fly ash; triaxial test

Citation: Manaviparast, H.R.; Pinheiro, J.; Najafi, E.K.; Abreu, C.; Araújo, N.; Cristelo, N.; Miranda, T. Mechanical Behavior of a Mine Tailing Stabilized with a Sustainable Binder. *Appl. Sci.* **2023**, *13*, 4103. https://doi.org/10.3390/app13074103

Academic Editor: Arcady Dyskin

Received: 7 March 2023
Revised: 20 March 2023
Accepted: 21 March 2023
Published: 23 March 2023

1. Introduction

Sustainable development is increasingly essential worldwide, and the study of innovative alternatives to long-used high environmental impact materials and products is essential to promote a more sustainable future [1]. The amount of mining waste generated worldwide makes this industry the top producer globally, with 5 to 7 billion tons produced annually [2]. Mine tailings can harm ecosystems due to their chemical, mineralogical composition, physical properties, and surface volume [3,4]. Tailings are considered acidic, especially those generated by metals such as copper and zinc; when placed in landfills, toxic elements are leached, creating severe risks of pollution to the environment. Hence, it is imperative to discover new methods to reuse excessive volumes of mining waste generated and deposited [5]. Additionally, the deposition of the tailings in landfills implies the need to increase the mechanical properties, generally performed by mixing the tailings with a conventional binder such as Portland cement.

Stabilizing mine tailings with Portland cement as a binder generates a high amount of carbon dioxide (CO_2); for each ton of Portland cement produced, a ton of CO_2 is generated, making the cement industry responsible for about 7% of the world's total greenhouse gas emissions [6]. Therefore, it is crucial to discover new sustainable solutions comparable to solutions that use Portland cement as a binder from a mechanical and environmental point of view. Consequently, chemical stabilization through the alkaline activation of industrial wastes has emerged. Alkaline activation (AA), also known as geopolymerization, is a chemical reaction produced by an aqueous solution, the mixture having materials as a solid

precursor rich in silica (SiO_2) and alumina (Al_2O_3) and an activator with high pH, based on sodium (Na) or potassium (K) [7]. Binders obtained by alkaline activation are a more sustainable solution in environmental terms and reduce the amount of emitted CO_2, e.g., using fly ash as a binder leads to a 45% reduction in CO_2 release compared to chemical stabilization with cement [8]. Generally, any material that contains a certain amount of alumina and silica is a potential precursor to being used in the AA process [9]. Most available aluminosilicates have a crystalline structure, making them stable to interact with any chemical reaction. However, the sources of aluminosilicates can be of natural origins, such as kaolins, resulting from a chemical process of feldspathic rocks undergoing heat treatment or industrial waste such as slag (obtained in blast furnaces), coal fly ash (thermal power plants), volcanic ash (heat treatment) and dust tiles or brick (industrial baking ovens) [10]. One proposed suggestion is the implementation of FA as a geopolymer binder since it is mainly composed of silica and alumina, in the amorphous state, with a shape and size favorable to AA [11]. In addition, FA is more susceptible to combination with alkaline activators based on sodium and potassium [12]. The polymeric gel originates immediately after the activator comes into contact with the silica/alumina source, having a Si/Al ratio of 1.0 [13–15]. The Si/Al ratio that best suits the use of fly ash as a precursor is 2.0 [16]. More homogeneous and dense reaction products form with an increase in Si/Al ratio [17]. The most frequently used chemical activators are sodium hydroxide (NaOH) and potassium hydroxide (KOH). The dose of the alkaline activator used is crucial and contributes to the hydration kinetics; impacting the hardening processes related to the strength of the geopolymer material and its durability [18,19]. Alkaline activation process using class F fly ash as a precursor and sodium hydroxide with 10, 12.5, and 15 molal concentrations as the activator was studied. It was concluded that for longer curing periods, the concentrations of 12.5 molal and 10 for shorter curing periods obtained the highest resistance values because of the more effective development of the structure of the resulting products [20]. Curing conditions involving mixtures with sodium silicate/sodium hydroxide and fly ash are not demanding in terms of temperature since they can be cured at room temperature, and it is necessary to ensure no water losses [12]. Alkaline activation with mine tailing indicates promising results regarding the immobilization of heavy metals [21]. However, the MT shows little reactivity in the geopolymerization process compared to other tailings, such as slag, fly ash, and metakaolin. Thus, it is necessary to use MT with a precursor rich in silica and alumina to increase the reaction reactivity and improve the properties of synthesized geopolymers [22–24].

This study aimed first to conduct geotechnical tests, including consistency limits, Proctor, CBR, uniaxial and permeability tests, and granulometric analysis to characterize the tailings. Then, triaxial tests were performed to evaluate the mechanical behavior of the mine tailings (MT) before and after stabilization with fly ash (FA). Chemical analyses on the mine tailing and fly ash using X-ray diffraction (XRD), X-ray fluorescence spectrometry (XRF) and also a study on conducted scanning electron microscopy (SEM) analyses were conducted.

2. Materials

2.1. Mine Tailing

The tailings of this study, as shown in Figure 1, came from the Neves Corvo mine located in the south of Portugal, provided by the Somincor company. After drying in an oven at a temperature of 110 °C, the tailings were broken down manually before testing.

The following tests were conducted to characterize the tailings: (a) the value of the liquidity limit (ω_l) through the Casagrande test was obtained equal to 23%; (b) the plasticity limit (ω_p) was obtained equal to 12%, and the plasticity index (I_P) was equal to 11%; (c) the density of solid particles was obtained using the IGPAI standard (1965) equal to 3.51; (d) the granulometric curve of the tailing under study was determined based on the LNEC (National Laboratory for Civil Engineering) specification (1966a). The grain size curve of the specimen is shown in Figure 2. The results obtained indicated the proportions of

sand (12%), silt (74.2%), and clay (13.8%) in the MT, showing that a large part of the tailing particles is the size of silt.

Figure 1. Mine tailing used in this study.

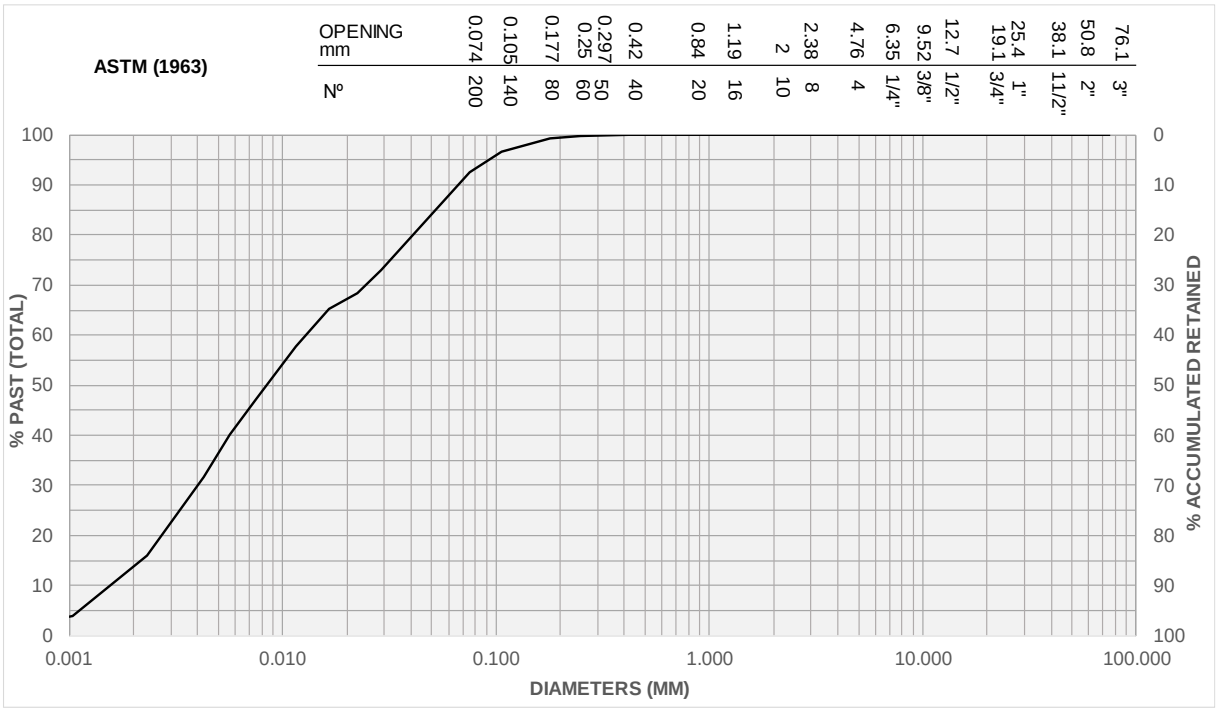

Figure 2. Grading curve of the mine tailing.

The tailing classification was performed according to the ASTM unified classification (2006). As the percentage that passed through the #200 sieve was greater than 50% ($P_{\#200}$ = 92.6%), the liquidity limit (ω_l) is equal to 23%, the plasticity index (I_p) is equal to 11%, and considering the tailing as an inorganic material, with a percentage retained on the #200 sieve less than 15%, the tailing was designated as CL—lean clay.

The Proctor test was carried out according to the LNEC specification (1966b). The modified Proctor test determined the optimal water content (ω_{opt}) of 11.0% and the maximum dry density mass ($\rho_{d,\,max}$) of 2.29 g/cm^3. The standard Proctor test determined the optimal water content (ω_{opt}) and maximum dry density ($\rho_{d,\,max}$) of 14.9% and 2.14 g/cm^3, respectively.

The CBR test was performed based on the LNEC specification (1967) to quantify the mechanical resistance of the tailing before and after saturation. The CBR values of 19% and

5% were obtained before and after the saturation of the specimen, respectively. It was found that the saturation of the tailings significantly affected its mechanical strength, resulting in very low CBR values.

The permeability test was carried out based on the BS 1377-5 (1990) standard. The specimen was built based on the optimal condition resulting from the standard proctor test. The obtained permeability coefficient was 10^{-7}cm/s. This value is typically associated with clayey soils [25,26].

The chemical, mineralogical and microstructural composition of the tailing were evaluated using XRD, XRF and SEM analysis. The XRD analysis was carried out at the electron microscopy unit of the University of Trás-os-Montes and Alto Douro. The XRF analysis was conducted at the Instituto de Ciências de la Construcción Eduardo Torroja in Madrid. Based on XRD analysis (Figure 3), the predominant characteristic minerals in the tailings, namely, pyrite (p = FeS_2), quartz (q = SiO_2), siderite (s = $FeCO_3$) and franklinite (f = $ZnFe_3 + 2O_4$), were observed. Two other elements are also highlighted, but their determination was not considered relevant due to the low percentages of the two minerals.

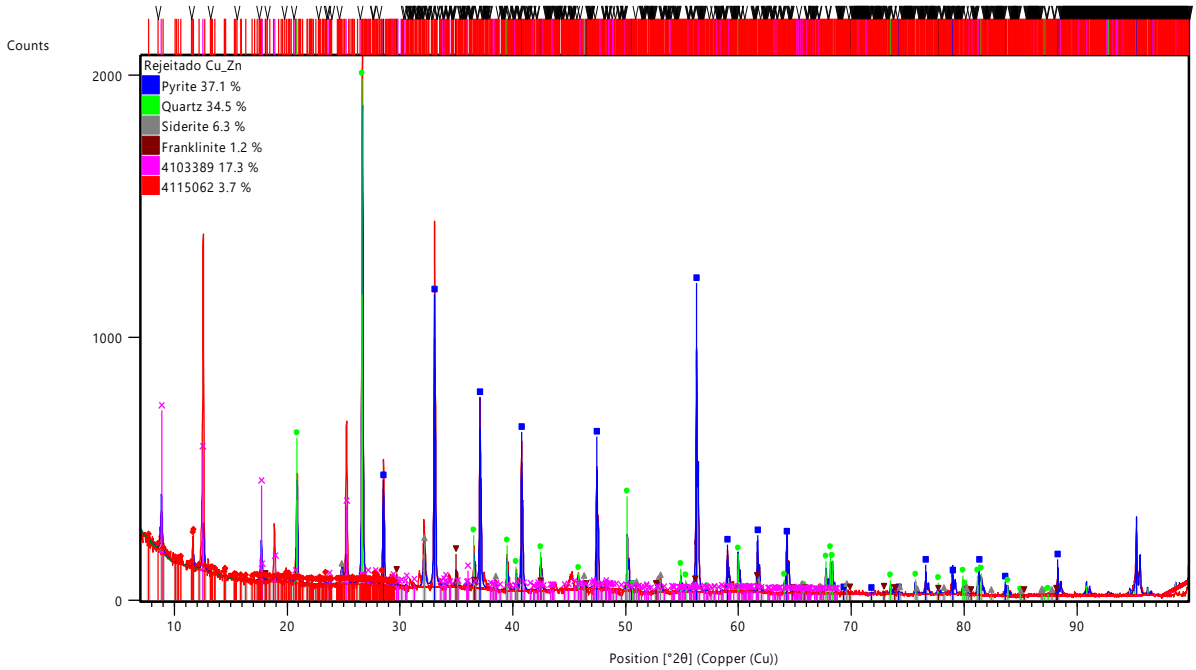

Figure 3. Mineralogical composition of the mine tailing obtained by XRD.

The XRF analysis evaluated the tailing composition (Table 1). It was verified that the predominant oxides in the tailings are sulfur (23.52%), silica (22.95%), iron (21.62%), carbon (19.30%) and aluminum (7.76%). Mine tailing contains some heavy metals in its composition, including arsenic (As), chromium (Cr), copper (Cu), manganese (Mn), lead (Pb) and zinc (Zn). These results confirm the strong reactivity of the tailing when exposed to oxidizing agents and the consequent high predisposition for the generation of acid mine drainage (AMD).

The microstructure of the mine tailing was evaluated by Coelho (2016) [27] using scanning electron microscopy (SEM), as shown in Figure 4. The results showed that the tailing presents a very irregular structure with different particle sizes and shapes.

Table 1. Chemical composition of the mine tailing obtained by XRF.

Oxides	Concentration (%)
Na_2O	0.42
MgO	1.47
Al_2O_3	7.76
SiO_2	22.95
P_2O_5	0.05
Cl	0.02
K_2O	0.66
MnO	0.08
CuO	0.22
Cr_2O_3	0.02
Fe_2O_3	21.62
CO_2	19.30
CaO	0.66
TiO_2	0.16
ZnO	0.51
As_2O_3	0.23
SO_3	23.52
PbO	0.35

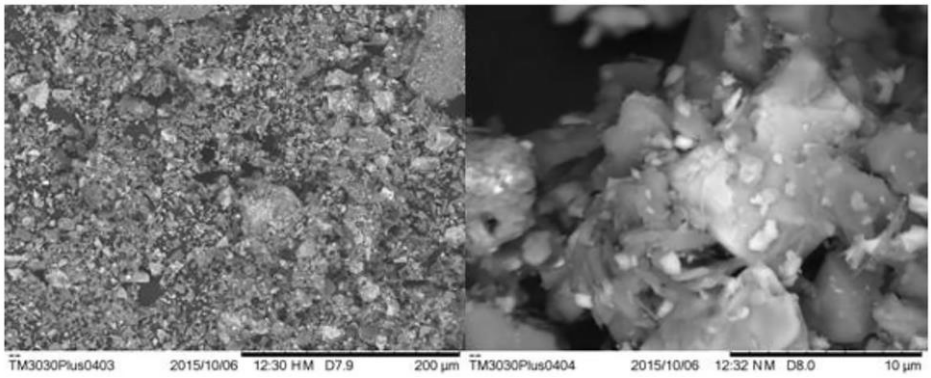

Figure 4. Microstructure of the mine tailing obtained through SEM by Coelho (2016) [27].

2.2. Fly Ash

Class F fly ash, as shown in Figure 5, was used as the precursor material in the alkaline activation process of the mine tailing, resulting from the combustion of mineral coal from the Pego thermoelectric power plant in Portugal. The chemical analysis of the fly ash (FA) is presented based on the work of Coelho (2016) [27]. The composition of the fly ash was evaluated using XRD, XRF and SEM analysis.

Figure 5. Class F fly ash used in this study.

The XRD analysis is shown in Figure 6 allowed to verify that FA comprises mullite minerals (mu = $3Al_2O_3SiO_2$) and quartz (q = SiO_2). The XRF analysis shown in Table 2 indicated that the predominant oxides in the FA are silica (51.50%), alumina (23.10%) and iron (23%). The high composition of silica and alumina confirms the predisposition of fly ash in the alkaline activation process, representing a source of available aluminosilicates (SiO_2 + Al_2O_3) of approximately 75%. Due to the reduced reactivity of the mine tailings (SiO_2 + Al_2O_3 = 30.71%), implementing fly ash as a precursor material is essential in developing the geopolymeric reactions for the alkaline activation process. Finally, the SEM images showed that the FA was regular, with tendentially spherical particles (Figure 7).

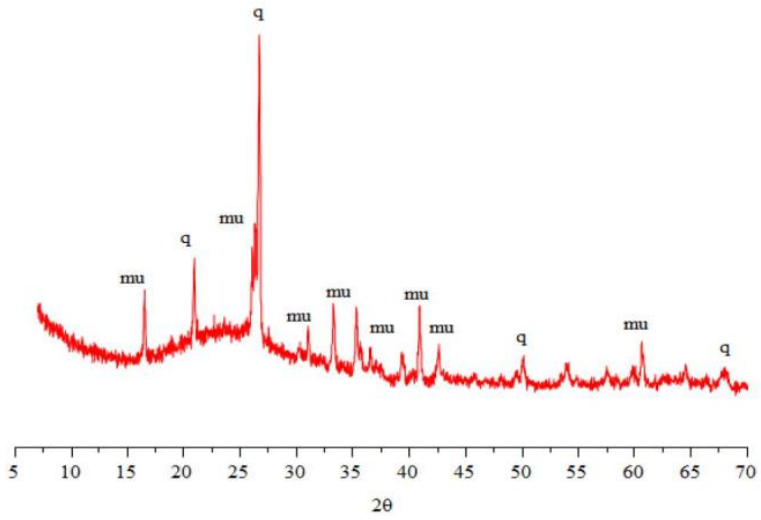

Figure 6. Mineralogical composition of the fly ash obtained by XRD.

Table 2. Chemical composition of the fly ash obtained by XRF.

Oxides	Concentration (%)
Al_2O_3	23.10
BaO	0.11
CaO	2.12
CuO	0.04
Fe_2O_3	12.80
K_2O	3.05
MgO	2.19
MnO	0.11
Na_2O	1.81
NiO	0.03
P_2O_5	0.28
PbO	0.03
Rb_2O	0.03
SO_3	1.25
SiO_2	51.50
SrO	0.08
TiO_2	1.49
ZnO	0.05
ZrO_2	0.05

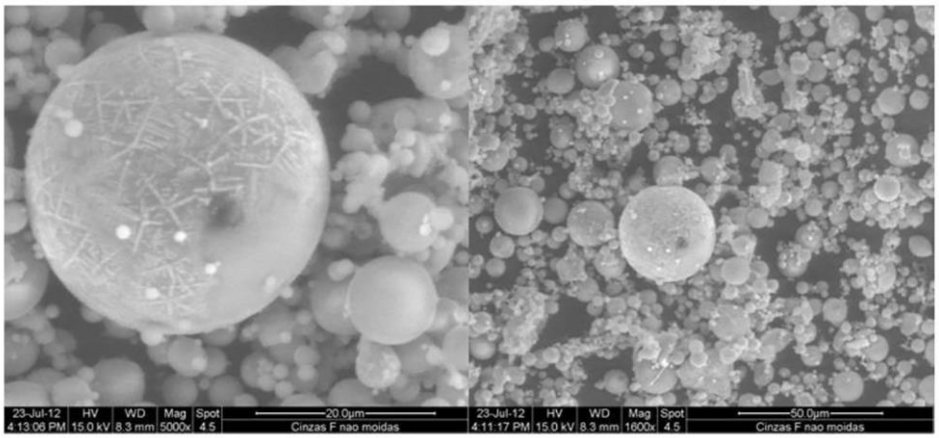

Figure 7. Microstructure of the fly ash obtained by SEM.

3. Experimental Program

3.1. Mechanical Behavior of the Mine Tailing before Stabilization

3.1.1. Preparation

The non-stabilized tailing specimens were constructed using a consolidometer. The specimens were prepared considering an initial water content of 30% and a dry density of 2.14 g/cm^3. This high water content was used to guarantee the saturation of the mixture and the absence of pre-consolidation. The sample was placed inside a cylindrical PVC tube, 68 mm in diameter and 195 mm in height. The mold was then placed inside a plastic container filled with water to maintain the specimen's saturation during consolidation. After stabilization of the specimen (3 or 4 days on average), it was removed from the mold and then placed in the triaxial chamber in its natural state to evaluate the mechanical behavior of the tailing.

3.1.2. Triaxial Compression Test

Triaxial compression tests were performed to determine the shear strength parameters of the mine tailings, including cohesion and friction angle. The tests were carried out based on the BS 1377-7 (1990) standard, considering three distinct test phases: saturation, consolidation, and shear.

During the saturation phase, the Skempton B parameter was calculated and had to be higher than 0.95 to make the specimens considered saturated. After this stage, the consolidation phase was followed by an increase in the confining stress (σ_3). The specimens were tested for confining stresses of 50 kPa, 100 kPa and 200 kPa in NC and OC conditions. The isotropic consolidation curve of the mine tailings was also obtained by increasing and decreasing the confining stress, starting by increasing σ_3 up to 500 kPa, gradually decreasing until it becomes null, and finally, increasing σ_3 to 700 kPa. These loading and unloading cycles made it possible to determine the compressibility, expansibility and recompressibility of the material under analysis.

After consolidating the specimens, the shear phase was carried out in undrained conditions with the pore pressure (Δu) (CU) measurement. The shear strength parameters were determined in terms of total (i.e., c and ϕ) and effective (i.e., c′ and ϕ') stresses. This phase was carried out through loading and unloading cycles for values of axial strain (ε_a) of 0.2%, 0.5%, 2% and 5%, respectively.

3.2. Results Analysis

3.2.1. Isotropic Consolidation Test

The isotropic consolidation curve (ICC) obtained is shown in Figure 8. The results show that the tailing is much less deformable in the unloading and reloading cycles than in the first loading cycle.

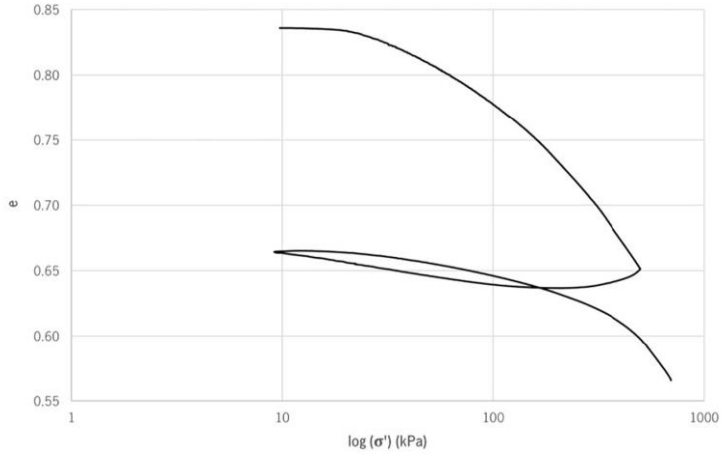

Figure 8. Isotropic consolidation curve of the mine tailing.

The critical states theory by Neves (2016) [26] was applied to determine the isotropic consolidation line and the critical states line (CSL). The volumetric compression of the tailings was evaluated until failure using the variation of the void index, expressed in terms of the specific volume (υ). This parameter was calculated based on Equation (1).

$$\upsilon = 1 + e \quad (1)$$

Figure 9 shows the delimitation of the isotropic compression and expansion lines.

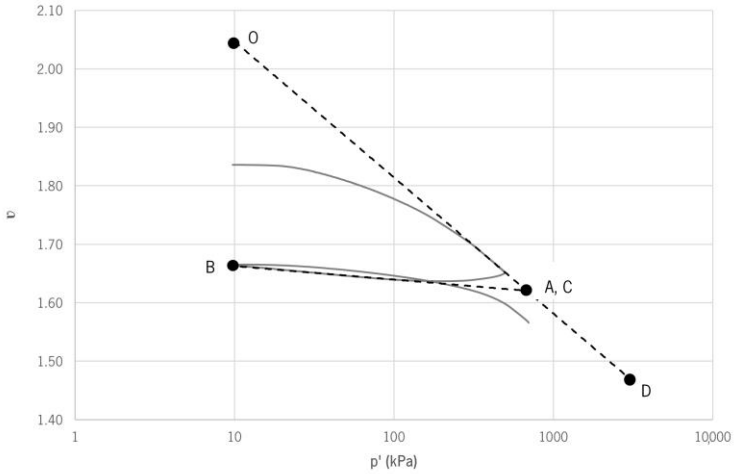

Figure 9. Isotropic compression and expansion curve.

The line OACD, corresponding to the first loading, is called the normal compression line (NCL) and is given by:

$$\upsilon = N - \lambda \ln (p') \quad (2)$$

where λ is the gradient and N is the value of υ for p′ = 1 kPa. The NCL of the mine tailing resulted in a value of λ = 0.101 and N = 2.2795. The BAC line is called the unloading–reloading line (also called the k-line) and is given by:

$$\upsilon = \upsilon_k - k \ln (p') \quad (3)$$

Similarly to the NCL parameters, k is the gradient, and υ_k is the value of υ for p′ = 1 kPa. The k-line of the mine tailing resulted in a k = 0.01 and υ_k = 1.6856.

Once the NCL was defined, the critical states line (CSL) was determined. The CSL was defined based on the failure points of the specimens submitted to triaxial compression

tests for confining the stresses of 50 kPa, 100 kPa and 200 (NC) kPa. The trajectory of the effective stresses in relation to the trajectory of the total stresses was represented in blue, according to the system (υ, ln (p′)). As the test was carried out in undrained conditions, the variation in the specific volume is null, and therefore, the trajectories result in horizontal straight lines. The resulting CSL is represented in Figure 10. As the specimens presented stress trajectories with different lengths, the CSL was defined based on an average of the trajectories of the three tested specimens (Figure 11). The stress trajectory for the specimen with σ_3 = 200 (OC) kPa is also represented in green. The failure trajectory of this specimen ended in the CSL. The CSL was defined based on Equation (4).

$$\upsilon_c = \Gamma - \lambda \ln (p_c') \quad (4)$$

where index c indicates ultimate failure, λ represents the gradient of the isotropic CSL and NCL, and Γ the value of υ_c for p′ = 1 kPa. The CSL of the mine tailings resulted in a value of λ = 0.102 and Γ = 2.2771.

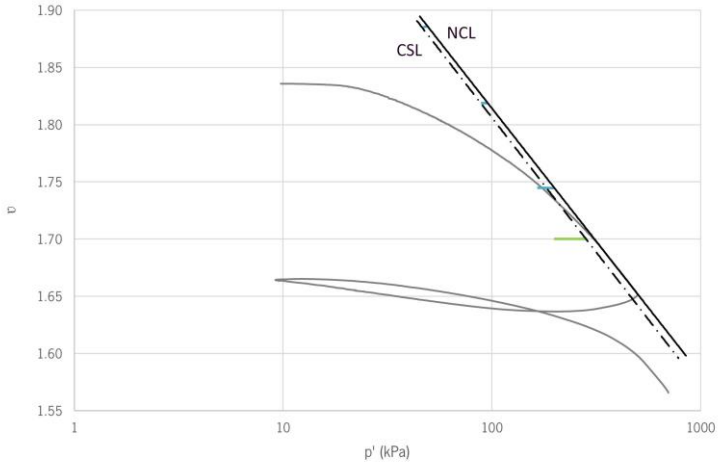

Figure 10. Isotropic consolidation curve with respective NCL and CSL.

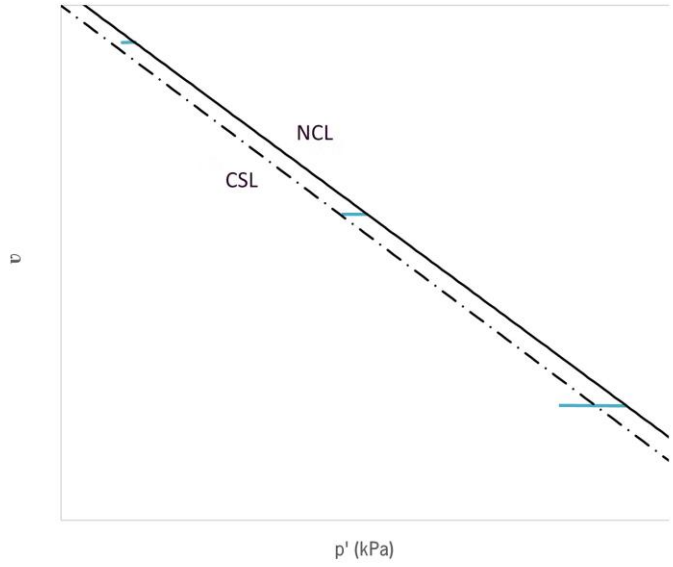

Figure 11. Detail of the stress trajectory and definition of the CSL.

Comparing the expressions determined for the NCL and the CSL, it is verified that the two lines are practically parallel since they present very similar gradient (λ) values. Furthermore, the value of N obtained is slightly higher than the value of Γ. The parameters

λ, Γ and k are constants and translate some intrinsic properties of the material under study. Neves (2016) [26] defined values for these critical state parameters for some typical soils (Table 3). Considering the values presented by the author, the critical state parameters defined that the mine tailing reasonably resembles the typical behavior of Santa Clara clay.

Table 3. Values of λ, Γ and k for typical soils.

Soil	λ	Γ	k
London clay	0.16	2.45	0.062
Kaolin	0.19	3.14	0.050
Glacial moraine	0.09	1.81	0.014
Santa Clara clay	0.10	1.94	0.011
River sand	0.16	2.99	0.014
Decomposed granite	0.09	2.04	0.005
Carbonate sand	0.34	4.35	0.003

3.2.2. CU Triaxial Tests

The evolution of the deviatoric stress (q) with the axial strain (ε_a) is shown in Figure 12. The analysis of the obtained results shows that the increase in the confining stress originated a respective increase in the values of q. For confining stresses of 50 kPa, 100 kPa and 200 kPa, the mine tailing showed typical behavior of a normally consolidated soil (NC), not showing peak deviatoric stresses, and with greater development of q between $0 < \varepsilon_a < 0.2\%$. During the shear phase, the specimen subjected to the OC ratio of 3.5 demonstrated a representative behavior of an overconsolidated soil, presenting a peak deviatoric stress (for $\varepsilon_a = 6.9\%$) and residual deviatoric stress. A greater evolution of q between $0 < \varepsilon_a < 0.5\%$ was observed for this specimen. This behavior can be explained by the fact that the overconsolidation of the specimens causes a greater rearrangement of the particles, which consequently causes a decrease in the void ratio and a respective increase in the mechanical strength of the specimen.

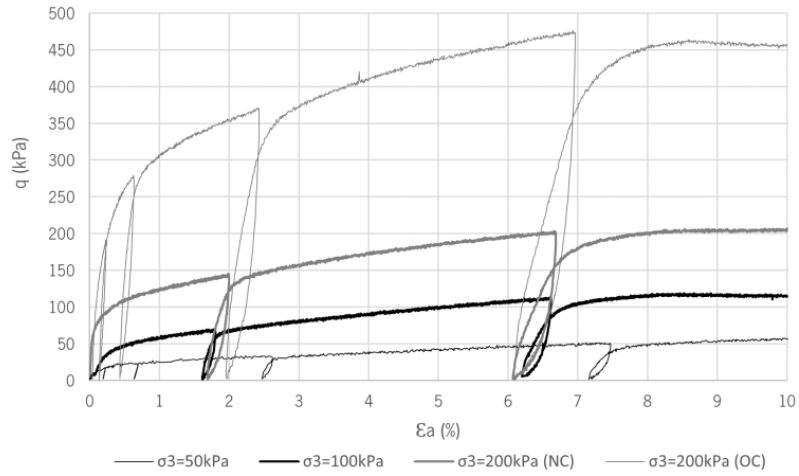

Figure 12. Evolution of the deviatoric stress with the axial strain.

Figure 13 shows the evolution of pore pressure (Δu) with axial strain (ε_a). It shows that the normally consolidated specimens present a contracting tendency with a positive evolution of the pore pressure throughout the shear phase. The overconsolidated specimen with $\sigma_3 = 200$ kPa exhibits a dilating behavior, whereby the pore pressure evolution curve lies below the curve for the normally consolidated specimen, subject to the same confining stress. The peaks observed along the curves are due to the loading/unloading cycles performed.

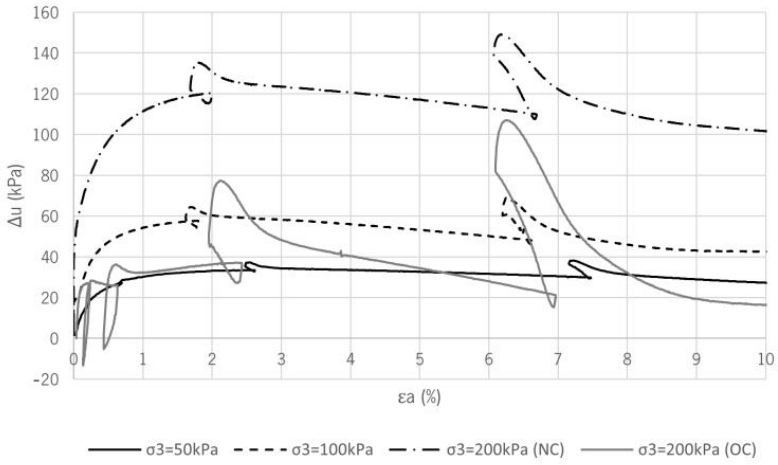

Figure 13. Evolution of pore pressure with axial strain.

Figure 14 shows the trajectories in terms of total and effective stresses.

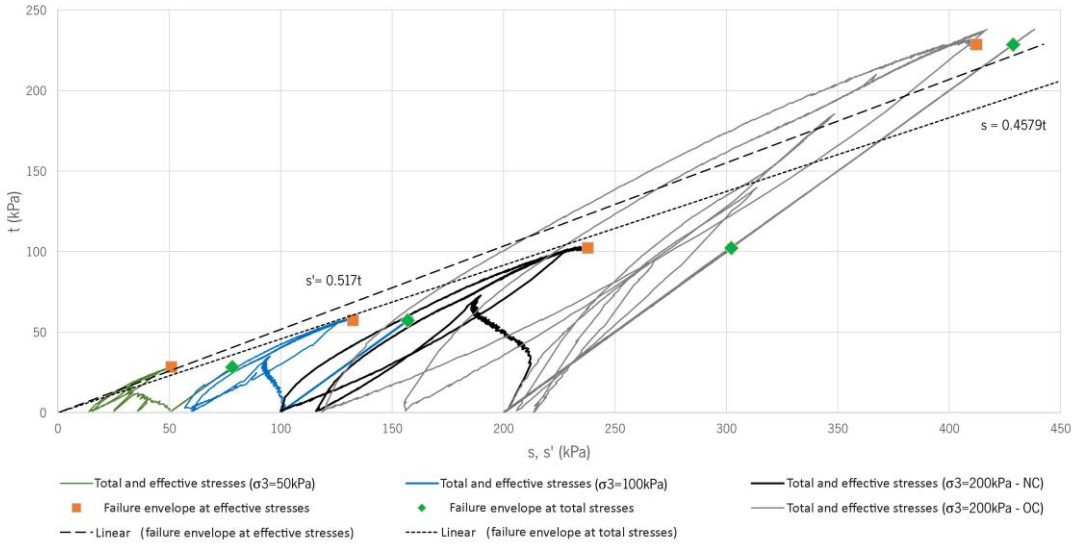

Figure 14. Mine tailing failure envelope.

The trajectory in terms of total stresses (s−t) is determined from the stresses imposed during the shear phase using Equations (5) and (6).

$$s = (\sigma_1 + \sigma_3)/2 \quad (5)$$

$$t = (\sigma_1 - \sigma_3)/2 \quad (6)$$

The trajectory in terms of effective stresses (s′–t) is obtained by reading pore pressure throughout the shear phase. During this phase, the increase in pore pressure is not linear, causing curvature of the effective stress path. For the normally consolidated specimens, in terms of effective stresses, a trajectory was observed with the stresses moving to the left. This development of stresses confirms the contracting behavior of these specimens. The overconsolidated specimen resulted in a trajectory of effective stresses with curvature tending to the right, highlighting the dilating tendency of this specimen. From these stress trajectories, the failure points were identified for each of the specimens tested, allowing us to trace the failure envelopes of the mine tailing in terms of total and effective stresses. The shear strength parameters of the specimens reconstituted from tailings were obtained

based on the deviatoric stresses of the specimens tested. Table 4 summarizes the shear strength parameters obtained (total cohesion (c), effective cohesion (c'), total friction angle (ϕ) and effective friction angle (ϕ') obtained from the resulting failure envelopes.

Table 4. Shear strength parameters of the mine tailing.

Total Stresses		Effective Stresses	
c	ϕ	c'	ϕ'
0	27°	0	31°

The strength parameters were calculated using Equations (7) and (8).

$$\tan \alpha = \sin \phi \quad (7)$$

$$c = a/\cos \phi \quad (8)$$

It was found that the mine tailing under study does not have undrained cohesion, in both total and effective stresses, since the samples were reconstituted in the laboratory.

4. Mechanical Behavior of Mine Tailing after Stabilization

4.1. Preparation

For all alkaline activation processes, an activator/fly ash ratio of 0.4 was used based on reports by Fernández-Jiménez et al., 2017 [28]. The concentration of NaOH used was 10 molal [29,30]. As shown in Table 5, three mixtures were defined, varying only in the amount of waste added to determine which mixture revealed a better mechanical performance.

Table 5. Composition of the mixtures studied (in grams and percentage).

	FA (g)	MT (g)	Activator (g)	Water (g)	NaOH (g)	FA (%)	MT (%)	Activator (%)	Water (%)
M1	500	500	200	142.9	57.1	50.0	50.0	16.7	11.9
M2	500	400	200	142.9	57.1	55.0	45.0	18.2	13.0
M3	500	600	200	142.9	57.1	45.0	55.0	15.4	11.0

Uniaxial Compression Tests

Uniaxial compression tests were performed according to the BS standard (1990). The tests were carried out with a constant displacement speed of 0.009 mm/s, using the triaxial compression test press with a 5 kN load cell. The displacements were measured using a linear variable differential transformer (LVDT). Three specimens were constructed for each of the three mixtures to evaluate the mechanical results in average terms. All specimens were tested on the same day, with a curing period of 7 days. This curing time does not allow a precise evaluation of the evolution of geopolymer reactions and characteristics of alkaline-activated mixtures in the long term. However, at this stage, it was only intended to determine which of the mixtures revealed a better mechanical performance.

The evolution of the compressive strength as a function of the axial strain of the specimens corresponding to mixtures M1, M2, and M3 was evaluated, as shown in Figure 15. In the first mixture (M1), the three specimens tested resulted in mechanical strengths of 482.8 kPa, 556.3 kPa, and 550.6 kPa, respectively. On average, the M1 mix resulted in a compressive strength of 529.9 kPa.

Regarding mixture M2, it was only possible to assess the behavior of one of the specimens since the two remaining were damaged during the test because the equipment used had supports with hinges, which caused the destabilization of the specimens seconds after the beginning of the test. For the M2 specimen, a compressive strength of 385.4 kPa was obtained.

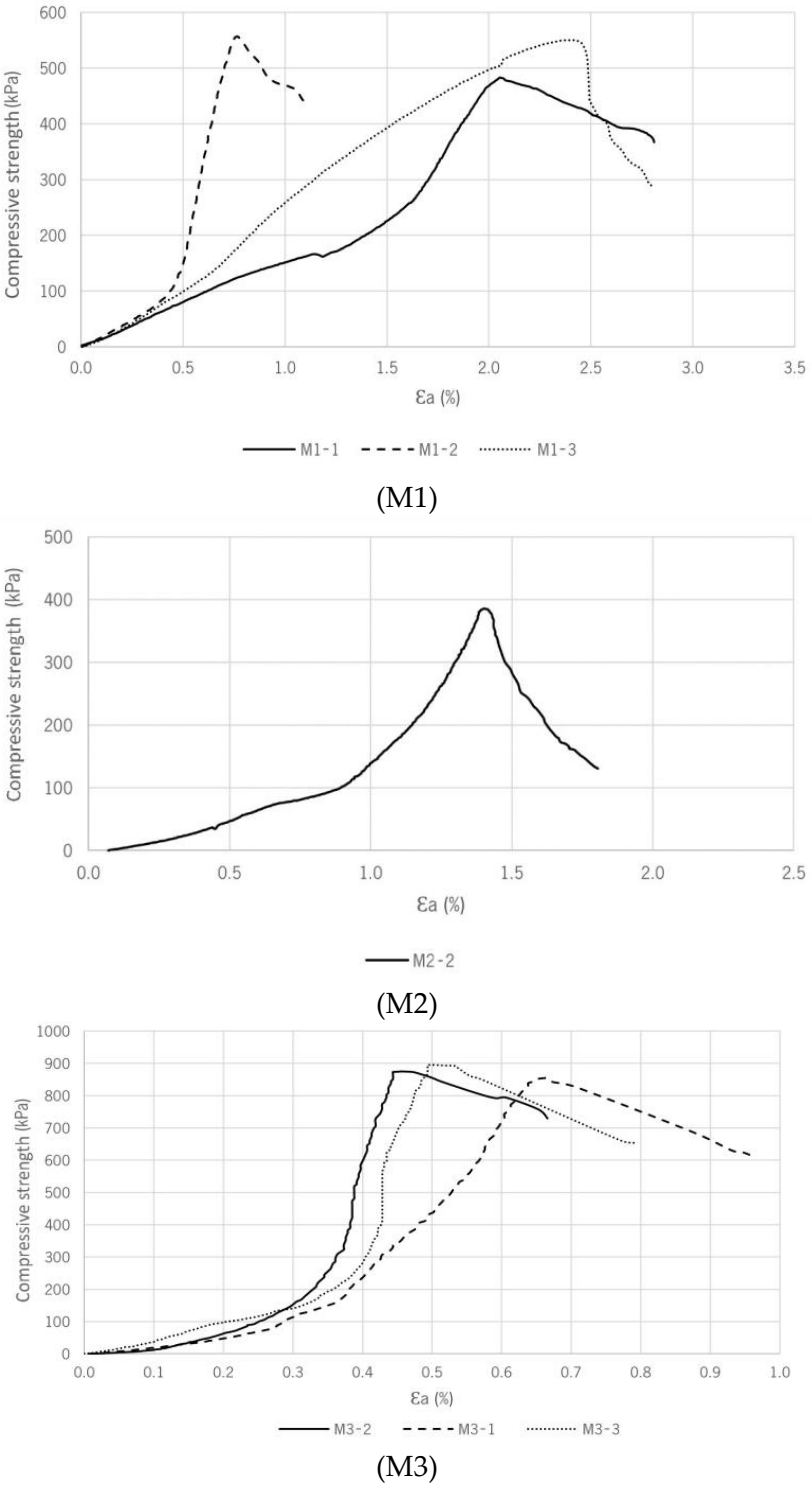

Figure 15. Evolution of compressive strength vs. axial strain for mixtures M1, M2 and M3.

For the last mixture defined (M3), the mechanical strengths achieved were 853.1kPa, 875.2 kPa, and 895.4 kPa, resulting in an average strength of 874.6 kPa. Among the mixtures studied, this was the most efficient. The mixture with the lowest amount of activator (M3) was the one that showed the best mechanical performance, meaning that the specimens of the two other mixtures (M1 and M2) were compacted with moisture contents higher than the optimum. In addition to demonstrating values with lower mechanical resistance, as they contain a greater amount of activator, mixtures M1 and M2 are less economical since

the cost associated with the production of the alkaline-activated cement resides in the cost of activating solutions.

4.2. Triaxial Compression Tests

The triaxial compression tests were carried out based on the BS 1377-7 (1990) standard. These tests were conducted to evaluate the shear strength, cohesion, and friction angle development of the mine tailing after stabilization. Only the mechanical behavior of the mixture M3, which revealed better mechanical performance based on the uniaxial compression test results, was evaluated. This mix comprises 55% mine tailing and 45% fly ash. All specimens were manufactured with 600 g of mine tailing, 500 g of fly ash and 200 g of sodium hydroxide in a concentration of 10 molal. All specimens were tested after 7 days of curing in a humid chamber at room temperature and with a relative humidity of 88%. The stabilized tailings specimens were consolidated with confining stresses of 50 kPa, 100 kPa, and 200 kPa. To obtain the ICC, the process adopted was the same as described for the unstabilized samples. This specimen was also submitted to the shearing for a tension of 200 kPa (test piece identified as σ_3 = 200′ kPa (OC)). The shear phase of all tested specimens was carried out under undrained conditions (UC) at the constant deformation rate of 2.74×10^{-4} mm/s.

4.3. Results Analysis

4.3.1. Isotropic Consolidation Test

The isotropic consolidation curves (ICC) obtained for the mine tailing in the original and stabilized state are shown in Figure 16, according to the system (log (σ′), e). It is observed that after the stabilization, the mine tailing presents a much lower evolution of the voids index during the loading, unloading and reloading phases. Similarly to what was observed in the ICC of the original tailing specimen, in the ICC of the stabilized tailing specimen, it was also verified that the tailing is less deformable in the trajectory of unloading and reloading than in the first loading cycle.

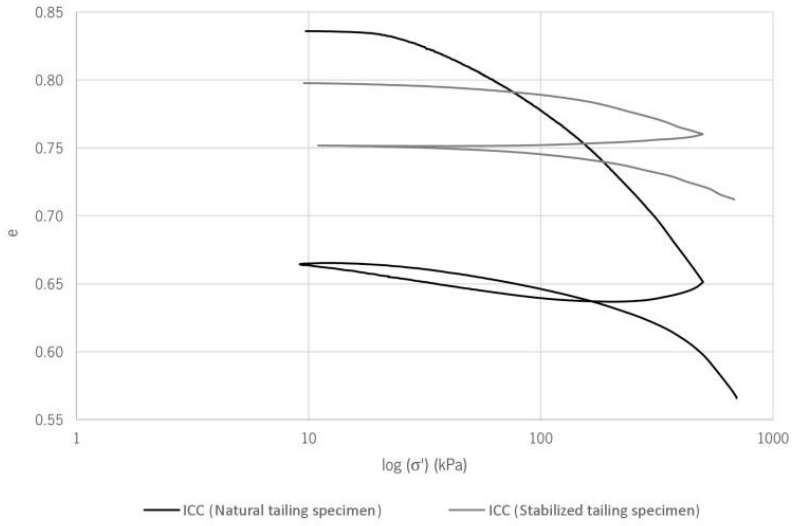

Figure 16. Isotropic consolidation curve of the mine tailing before and after stabilization.

The critical states theory was again applied using the fundaments presented by Neves (2016) [26] from the isotropic consolidation curve obtained for the improved tailing specimen. To determine the isotropic consolidation line and the critical states line (CSL), the ICC was made according to the coordinate system (p′, υ). Figure 17 shows the delimitation of the isotropic compression and expansion lines. The normal compression line (line O′A′C′D′) resulted in a value of λ = 0.024 and N = 1.91, resulting in Equation (18). The isotropic expansion line (line B′A′C′) resulted in a k = 0.00038 and υ_k = 1.7526.

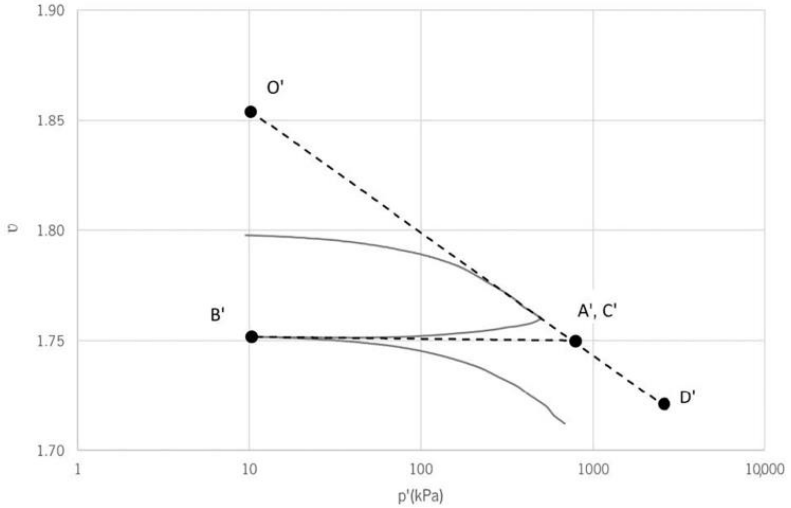

Figure 17. Isotropic compression and expansion curve (stabilized specimen).

Then, the CSL of the mine tailing after improvement was determined from the stress trajectory of the specimen used to obtain the ICC, in blue, whose initial void ratio was obtained. For the definition of the CSL, it was assumed that this line must be parallel to the NCL. The resulting CSL is represented in Figure 18, with a value of $\lambda = 0.024$ and $\Gamma = 1.8705$. Once the CSL was determined, the stress trajectory of the remaining specimens was represented, subjected to confining stresses of 50 kPa, 100 kPa and 200 kPa, in green, showing that they do not go beyond the NCL.

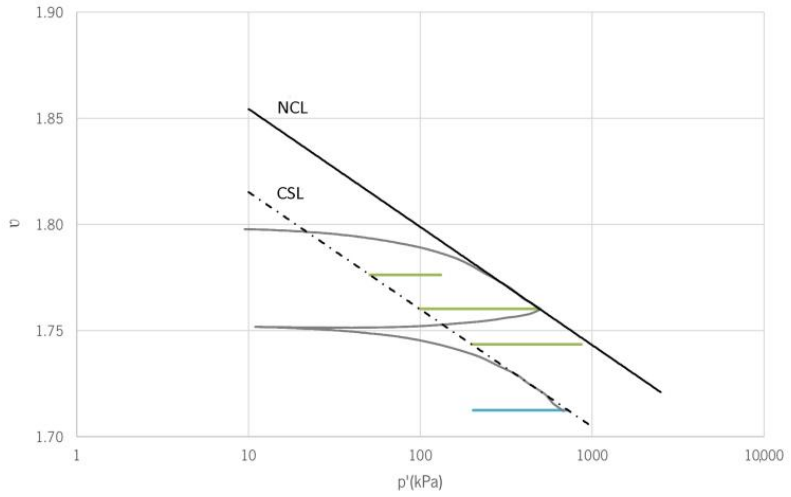

Figure 18. Isotropic consolidation curve with respective NCL and CSL (stabilized MT).

Table 6 presents the resulting parameters of the critical states theory before and after the stabilization of the mine tailings. The obtained parameters revealed notable differences, resulting in significantly lower values after the chemical stabilization by alkaline activation of the tailing. Regarding the NCL obtained for the original and stabilized tailing, the value of λ decreased about 4.2 times (76%), and the value of N decreased about 1.2 times (16%). Comparing the CSL parameters, the values of λ and Γ also reduced by about 76% and 16% after stabilization. Finally, by evaluating the variation of the unloading–reloading line parameters (k-line), a decrease in the value of k of about 26.3 times (96%) was observed. However, a slight increase in the value of υ_k, by around 4%, was observed.

Table 6. Parameters of the critical states theory before and after stabilization.

Parameters	NCL		CSL		K-Line	
	λ	N	λ	Γ	k	υ_k
Natural MT	0.101	2.2795	0.102	2.2771	0.01000	1.6856
Stabilized MT	0.024	1.9100	0.024	1.8705	0.00038	1.7526

4.3.2. CU Triaxial Tests

The evolution of the deviatoric stress (q) with the axial strain (ε_a) for the alkaline-activated tailings specimens is shown in Figure 19. The increase in the confining stress resulted in a respective increase in the q values. The values of q obtained for stabilized specimens resulted in considerably higher resistances, showing the effects of the geopolymerization mechanism on the mechanical resistance of the mine tailing. All the specimens showed a peak and residual deviatoric stress, with greater development of q between $0 < \varepsilon_a < 0.2\%$, except for the specimen subjected to a confining stress of 200 kPa, whose test was interrupted with an axial strain level of 4.5%, due to a break in the laboratory's electrical supply. From the comparison of the failure stresses resulting from the uniaxial tests and the peak deviatoric stresses resulting from the triaxial tests, both carried out in specimens with a curing period of 7 days, it is possible to observe the influence of the application of different confining stresses. The stabilized samples with the alkaline cement submitted to different values of σ_3 revealed much higher peak deviatoric stresses than the failure stresses obtained through uniaxial tests, highlighting the impact of confining stress on the strength of the tailing–binder mixtures.

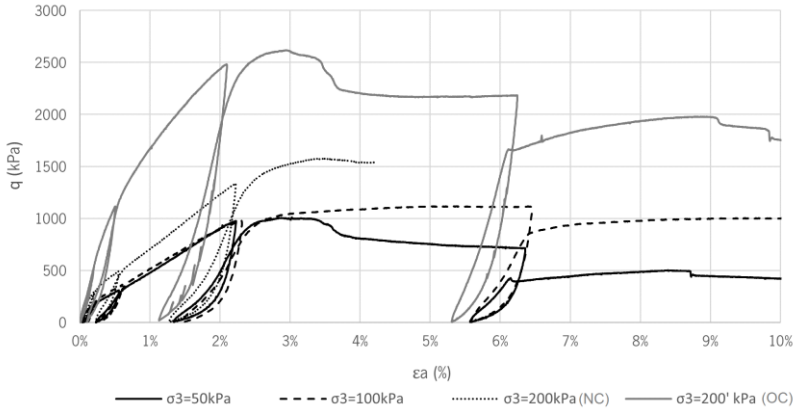

Figure 19. Evolution of the deviator stress with axial strain (stabilized specimens).

Figure 20 shows the evolution of pore pressure (Δu) with axial strain (ε_a) for the improved specimens. It was observed that all specimens showed an overconsolidation-typical behavior, showing a contracting tendency ($\Delta u > 0$) during the first phase of the test and a dilating tendency ($\Delta u < 0$) during the rest of the test. This behavior indicates that the specimens manifest an excess of pore pressure until the development of their maximum mechanical resistance up to failure, followed by the dissipation of the excess pore pressure and consequent dilation of the specimens. The peaks observed along the curves are due to the loading and unloading cycles performed.

Figures 21 and 22 show the resulting stress trajectories regarding total and effective stresses. It can be observed that for all the specimens, in terms of effective stresses, the trajectories tend to the right. This stress development confirms the overconsolidation and the dilating behavior of these specimens. From the stress trajectories, the failure points of each of the specimens were identified once again, thus allowing us to trace the failure envelopes of the stabilized mine tailings. This analysis was performed for peak and

residual deviatoric stresses. Tables 7 and 8 summarize the shear strength parameters (total cohesion (c), effective cohesion (c′), total friction angle (ϕ) and effective friction angle (ϕ′)) determined from the resulting failure envelopes. Comparing the shear strength parameters obtained before and after stabilizing the mine tailings, a significant evolution was verified. Concerning cohesion, both in total and effective stresses, the value remained zero for the original and improved tailing. This fact shows that 7 days of curing is insufficient to develop significant bonding between the binder and the solid particles.

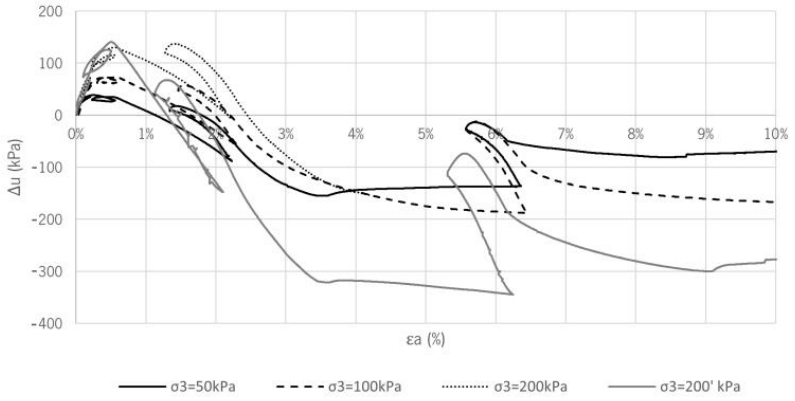

Figure 20. Evolution of pore pressure with axial strain (stabilized specimens).

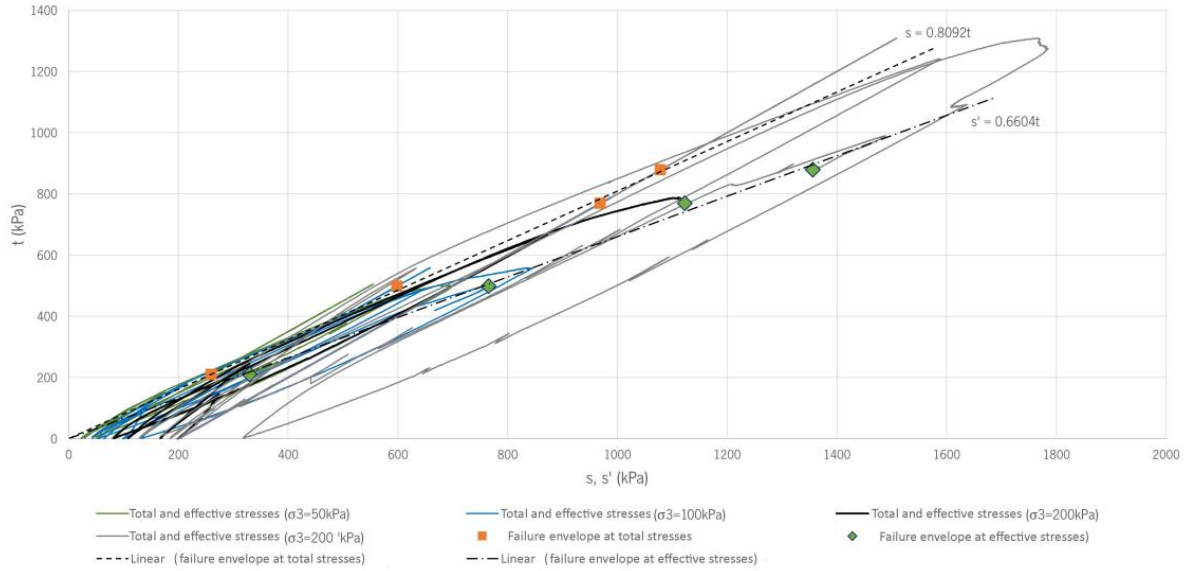

Figure 21. Failure envelopes of the mine tailing in residual deviatoric stresses (stabilized specimens).

Table 7. Shear strength parameters of the mine tailing before and after stabilization (residual deviatoric stresses).

	Total Stresses		Effective Stresses	
	c	**ϕ**	**c′**	**ϕ′**
Natural MT	0	27°	0	31°
Stabilized MT	0	54°	0	41°

Table 8. Shear strength parameters of the mine tailing before and after stabilization (peak deviatoric stresses).

	Total Stresses		Effective Stresses	
	c	**ϕ**	**c′**	**ϕ′**
Natural MT	0	27°	0	31°
Stabilized MT	0	58°	0	46°

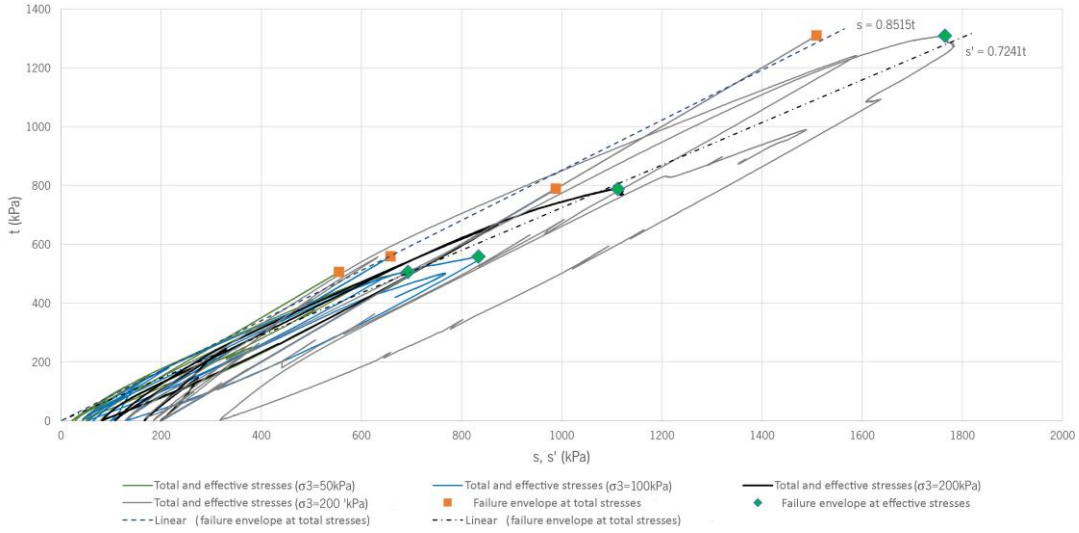

Figure 22. Failure envelopes of the mine tailing in peak deviatoric stresses (stabilized specimens).

However, there was a considerable increase in the friction angle, both in total and effective stresses, for the tailing–binder mixture studied. The considerable increase in the friction angle after the stabilization of the tailings may be related to the addition of a considerable percentage of fly ash to the mixture, which contributes to a better filling of the voids existing between the particles of tailings, resulting in a more compacted matrix, with the consequent increase in the friction angle.

5. Conclusions

The deposition of tailings resulting from the mining operation in landfills must be better managed since these tailings, in contact with erosive agents such as air and water, release chemical elements forming acid mine drainage. Additionally, their mechanical properties must be improved many times for safer disposal in landfills. These tailings are normally stabilized with Portland cement. However, there are very high environmental impacts associated with the production of Portland cement, and more sustainable solutions are needed. This study evaluated the improvement of the mechanical characteristics of a mine tailing using a sustainable binder obtained through the alkaline activation of fly ash.

The mine tailing was initially submitted to a series of geotechnical characterization tests. Based on the results obtained, the mine tailing was classified as lean clay (CL). Based on the theory of critical states, the parameters that allow the delimitation of the NCL, k-line and CSL were defined. The obtained results indicated that the critical state parameters of the mine tailings are reasonably similar to the typical values of Santa Clara clay.

Concerning the process of improving mine tailings using an alkaline activation technique, the composition of tailing–binder mixtures was defined. Through uniaxial compression tests, it was concluded that the mix with the best performance had the lowest moisture content (55% tailing + 45% fly ash). The most promising mixture was evaluated using triaxial compression tests in both unstabilized and stabilized samples. The stabilization process by alkaline activation significantly influenced the shear strength of the tailing. In

fact, even for a short curing period (7 days), a significant increase in friction angle was observed even though cohesion maintained zero value since this period is not enough to develop measurable bonds between the binder and the solid particles. In this sense, the shear strength is expected to increase significantly with the curing time, namely with the increase in cohesion.

From the theory of critical states, there was a notable reduction in the parameters that define the NCL, k-line, and CSL, showing a considerable reduction in compressibility and recompressibility for the stabilized specimens.

In short, this study characterized the mechanical behavior of the mine tailing before and after stabilization with a sustainable binder based on the alkaline activation of fly ash. The mechanical properties increase due to the development of a binder due to the alkaline activation of the fly ash that reacted with the activator. The results showed the efficacy of the stabilization treatment in the increase in the shear strength of the mine tailing, even for a short-term curing period.

Author Contributions: Conceptualization, H.R.M., J.P., E.K.N., C.A., N.A., N.C. and T.M.; methodology, H.R.M., J.P., E.K.N., C.A., N.A., N.C. and T.M.; formal analysis, H.R.M., J.P. and T.M.; investigation, H.R.M., J.P., C.A. and T.M.; resources, N.A., N.C. and T.M.; writing—original draft, H.R.M.; writing—review and editing, H.R.M., J.P., E.K.N., C.A., N.A., N.C. and T.M.; supervision, N.A., N.C. and T.M.; project administration, N.C. and T.M.; funding acquisition, N.C. and T.M. All authors have read and agreed to the published version of the manuscript.

Funding: This work was partly financed by FCT/MCTES through national funds (PIDDAC) under the R&D Unit Institute for Sustainability and Innovation in Structural Engineering (ISISE), under reference UIDB/04029/2020, and under the Associate Laboratory Advanced Production and Intelligent Systems ARISE under reference LA/P/0112/2020. This work was also partly funded by the research project MINECO—New Eco-Innovative Materials for Mining Infra, with reference ERA-MIN/0001/2018, funded by Portuguese State Budget through the FCT/MCTES.

Institutional Review Board Statement: This study did not require ethical approval.

Informed Consent Statement: This study did not involve humans.

Data Availability Statement: Not available data.

Acknowledgments: The authors would like to thank FCT/MCTES for funding the project MINECO—New Eco-Innovative Materials for Mining Infra, with reference ERA-MIN/0001/2018.

Conflicts of Interest: The authors declare no conflict of interest.

References

1. Evans, D.L.; Janes-Bassett, V.; Borrelli, P.; Chenu, C.; Ferreira, C.S.; Griffiths, R.I.; Kalantari, Z.; Keesstra, S.; Lal, R.; Panagos, P. Sustainable Futures over the next Decade Are Rooted in Soil Science. *Eur. J. Soil Sci.* **2022**, *73*, e13145. [CrossRef]
2. Marin, O.A.; Kraslawski, A.; Cisternas, L.A. Estimating Processing Cost for the Recovery of Valuable Elements from Mine Tailings Using Dimensional Analysis. *Miner. Eng.* **2022**, *184*, 107629. [CrossRef]
3. Almeida, J.; Faria, P.; Ribeiro, A.B.; Silva, A.S. Effect of Mining Residues Treated with an Electrodialytic Technology on Cement-Based Mortars. *Clean. Eng. Technol.* **2020**, *1*, 100001. [CrossRef]
4. Song, X.; Pettersen, J.B.; Pedersen, K.B.; Røberg, S. Comparative Life Cycle Assessment of Tailings Management and Energy Scenarios for a Copper Ore Mine: A Case Study in Northern Norway. *J. Clean. Prod.* **2017**, *164*, 892–904. [CrossRef]
5. Perumal, P.; Niu, H.; Kiventerä, J.; Kinnunen, P.; Illikainen, M. Upcycling of Mechanically Treated Silicate Mine Tailings as Alkali Activated Binders. *Miner. Eng.* **2020**, *158*, 106587. [CrossRef]
6. Izumi, Y.; Iizuka, A.; Ho, H.-J. Calculation of Greenhouse Gas Emissions for a Carbon Recycling System Using Mineral Carbon Capture and Utilization Technology in the Cement Industry. *J. Clean. Prod.* **2021**, *312*, 127618. [CrossRef]
7. Abreu, C.I.G. Melhoramento de Rejeitado Mineiro através de Ligantes Sustentáveis. Master's Thesis, University of Minho, Braga, Portugal, 2022.
8. Provis, J.L.; Palomo, A.; Shi, C. Advances in Understanding Alkali-Activated Materials. *Cem. Concr. Res.* **2015**, *78*, 110–125. [CrossRef]
9. Khalifa, A.Z.; Pontikes, Y.; Elsen, J.; Cizer, Ö. Comparing the Reactivity of Different Natural Clays under Thermal and Alkali Activation. *RILEM Tech. Lett.* **2019**, *4*, 74–80. [CrossRef]

10. Da Silva, M.C.A. Melhoramento de um Solo Argiloso com Recurso à Ativação Alcalina de Resíduos para Aplicação em Infraestruturas de Transporte. Master's Thesis, University of Minho, Braga, Portugal, 2016.
11. Toniolo, N.; Boccaccini, A.R. Fly Ash-Based Geopolymers Containing Added Silicate Waste. A Review. *Ceram. Int.* **2017**, *43*, 14545–14551. [CrossRef]
12. Cristelo, N.; Glendinning, S.; Teixeira Pinto, A. Deep Soft Soil Improvement by Alkaline Activation. *Proc. Inst. Civ. Eng. -Ground Improv.* **2011**, *164*, 73–82. [CrossRef]
13. Criado, M.; Fernández-Jiménez, A.; Palomo, A. Alkali Activation of Fly Ash: Effect of the SiO_2/Na_2O Ratio: Part I: FTIR Study. *Microporous Mesoporous Mater.* **2007**, *106*, 180–191. [CrossRef]
14. Fernández-Jiménez, A.; Palomo, A. Composition and Microstructure of Alkali Activated Fly Ash Binder: Effect of the Activator. *Cem. Concr. Res.* **2005**, *35*, 1984–1992. [CrossRef]
15. Provis, J.L. Geopolymers and Other Alkali Activated Materials: Why, How, and What? *Mater. Struct.* **2014**, *47*, 11–25. [CrossRef]
16. Wang, J.; Wu, X.; Wang, J.; Liu, C.; Lai, Y.; Hong, Z.; Zheng, J. Hydrothermal Synthesis and Characterization of Alkali-Activated Slag–Fly Ash–Metakaolin Cementitious Materials. *Microporous Mesoporous Mater.* **2012**, *155*, 186–191. [CrossRef]
17. Duxson, P.; Provis, J.L.; Lukey, G.C.; Separovic, F.; van Deventer, J.S. 29Si NMR Study of Structural Ordering in Aluminosilicate Geopolymer Gels. *Langmuir* **2005**, *21*, 3028–3036. [CrossRef]
18. Bílek, V.; Hrubỳ, P.; Iliushchenko, V.; Koplík, J.; Křikala, J.; Marko, M.; Hajzler, J.; Kalina, L. Experimental Study of Slag Changes during the Very Early Stages of Its Alkaline Activation. *Materials* **2022**, *15*, 231. [CrossRef]
19. De Oliveira, L.B.; de Azevedo, A.R.G.; Marvila, M.T.; Pereira, E.C.; Fediuk, R.; Vieira, C.M.F. Durability of Geopolymers with Industrial Waste. *Case Stud. Constr. Mater.* **2022**, *16*, e00839. [CrossRef]
20. Cristelo, N.; Glendinning, S.; Fernandes, L.; Pinto, A.T. Effects of Alkaline-Activated Fly Ash and Portland Cement on Soft Soil Stabilisation. *Acta Geotech.* **2013**, *8*, 395–405. [CrossRef]
21. Rao, F.; Liu, Q. Geopolymerization and Its Potential Application in Mine Tailings Consolidation: A Review. *Miner. Process Extr. Metall. Rev.* **2015**, *36*, 399–409. [CrossRef]
22. Pacheco-Torgal, F.; Castro-Gomes, J.P.; Jalali, S. Investigations of Tungsten Mine Waste Geopolymeric Binder: Strength and Microstructure. *Constr. Build. Mater.* **2008**, *22*, 2212–2219. [CrossRef]
23. Xiaolong, Z.; Shiyu, Z.; Hui, L.; Yingliang, Z. Disposal of Mine Tailings via Geopolymerization. *J. Clean. Prod.* **2021**, *284*, 124756. [CrossRef]
24. Akinyemi, B.A.; Alaba, P.A.; Rashedi, A. Selected Performance of Alkali-Activated Mine Tailings as Cementitious Composites: A Review. *J. Build. Eng.* **2022**, *50*, 104154. [CrossRef]
25. Smith, I.M. *Smith's Elements of Soil Mechanics*, 8th ed.; Blackwell Pub: Oxford, UK; Malden, MA, USA, 2006; ISBN 978-1-4051-3370-8.
26. Neves, E.M. *Mecânica dos Estados Críticos: Solos Saturados e Não Saturados*; ISTPress-Loja IST: Lisboa, Portugal, 2016; ISBN 978-9898481481.
27. Coelho, J. Utilização de Rejeitado da Mina de Neves Corvo no Fabrico de Misturas Geopoliméricas para Aplicações Geocténicas. Master's Thesis, University of Trás-os-Montes and Alto Douro, Vila Real, Portugal, 2016.
28. Santamaria-Fernandez, M.; Molinuevo-Salces, B.; Kiel, P.; Steenfeldt, S.; Uellendahl, H.; Lübeck, M. Lactic Acid Fermentation for Refining Proteins from Green Crops and Obtaining a High Quality Feed Product for Monogastric Animals. *J. Clean. Prod.* **2017**, *162*, 875–881. [CrossRef]
29. Abbas, M.M.; Rasheed, M. Solid State Reaction Synthesis and Characterization of Cu Doped TiO_2 Nanomaterials. *J. Phys. Conf. Ser.* **2021**, *1795*, 012059. [CrossRef]
30. Enneffatia, M.; Rasheed, M.; Louatia, B.; Guidaraa, K.; Shihab, S.; Barillé, R. Investigation of Structural, Morphology, Optical Properties and Electrical Transport Conduction of Li0.25Na0.75CdVO4 Compound. *J. Phys. Conf. Ser.* **2021**, *1795*, 012050. [CrossRef]